Bone Phenotype of Toll-like Receptor 5 Deficient (TLR5KO) Mice and PTH Treated Osteopenic Sheep

A Thesis

Presented to the Faculty of the Graduate School

of Cornell University

In Partial Fulfillment of the Requirements for the Degree of

Master of Science

by

Remy Elisabeth Walk

August 2017

© 2017 Remy Elisabeth Walk

ABSTRACT

Bone mass and mechanical properties are known to influence risk of fragility fracture. Clinical measures of bone mineral density (BMD) are used to evaluate fracture risk, but patients with obesity have greater risk of fracture than would be expected from BMD. Obesity is a common component of metabolic syndrome. Metabolic syndrome may contribute to the increased risk of fracture associated with obesity. Patients with osteoporosis have low bone mass and increased risk of fracture. Parathyroid hormone (PTH) treatment can be used to reverse the effects of osteoporosis. Here, we looked at mechanical properties of bone in an animal model of metabolic syndrome and an animal model of osteoporosis treated with parathyroid hormone.

First, we characterized the cortical bone phenotype of the toll-like receptor 5 deficient mouse (TLR5KO). The TLR5KO mouse is a model of metabolic syndrome with mild levels of adiposity. Metabolic syndrome in TLR5KO mice is caused by alterations to the gut microbiome. Male and female mice 10-55 weeks of age (n = 5-19/ group) were used in this study. Cortical bone geometry and mechanical properties of the mid-diaphysis of the femur were analyzed to characterize the cortical bone phenotype. The femurs were tested in three-point bending to obtain peak moment, bending rigidity and post yield displacement. Peak moment was related to geometry to infer the effect of genotype on tissue material properties. We found that metabolic syndrome was associated with impaired cortical bone tissue material properties in both male and female mice in most ages studied. In summary, metabolic syndrome with only mild adiposity was associated with alterations to bone strength that could not be explained by bone geometry and density, suggesting altered bone tissue material properties.

Secondly, we determined the mechanical properties of cancellous bone from osteopenic sheep treated with PTH. Osteopenia was induced in 6-7 year-old sheep through a combination of ovariectomy (OVX) and a diet to induce metabolic acidosis (MA). A year after OVX, the sheep

were treated with either vehicle (n = 6) or PTH (n = 7) for a year. Cancellous bone cores were taken from the medial caudal quadrant of the right distal femur for mechanical testing. We found no detectable effect of PTH treatment on mechanical properties of cancellous bone in uniaxial compression.

BIOGRAPHICAL SKETCH

Remy Elisabeth Walk was born in Wynnewood, Pennsylvania in 1992. She graduated from The Baldwin School in 2011. In 2015, she graduated cum laude from Cornell University in Ithaca, New York with a Bachelor of Science degree in Mechanical Engineering.

ACKNOWLEDGMENTS

I would like to thank my friends and family for their support and encouragement. I would also like to thank my graduate advisory committee for their help and guidance. In addition, the advice and assistance of the entire Hernandez Lab was invaluable in the completion of this thesis.

TABLE OF CONTENTS

CHAPTER 1

INTRODUCTION

1.1 Bone

Bone is a hierarchical composite material with components consisting of mineral, organic molecules and water. At the millimeter scale, we observe two types of bone: cortical and trabecular (cancellous) bone (Fig. 1.1).

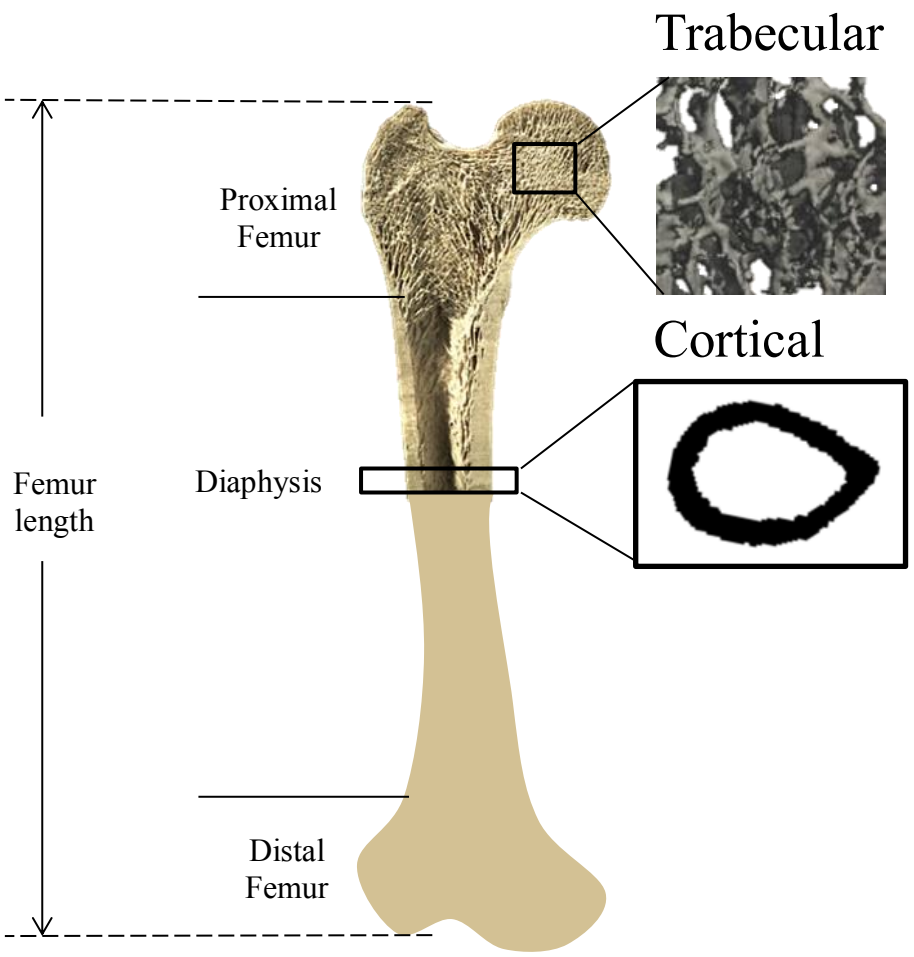

Figure 1.1: In long bones such as the femur shown, trabecular and cortical bone are found. Femur length is measured from the lateral condyle to the greater trochanter.

Cortical bone is the dense (5-10% porosity) outer shell and shaft of long bones such as the femur. Trabecular bone is much more porous than cortical bone and is located in the ends of long bones and the majority of the vertebra. The trabeculae of cancellous bone generally align with the directions of principal stress.

1.2 Fragility Fracture and Whole Bone Mechanical Properties

A fracture caused by a low level trauma such as a fall from standing height is known as a fragility fracture [1]. Clinically, bone mineral density (BMD), measured using dual-energy X-ray absorptiometry (DXA), provides an estimate of fracture risk. An increase in BMD is associated with a decrease in fracture risk; however, there are populations in which fracture risk exceeds what is expected from BMD. To understand fracture risk not explained by BMD, we can assess whole bone mechanical properties. Whole bone mechanical properties are determined by bone morphology and tissue material properties [2].

Bone morphology refers to the shape of the bone. The diaphysis of long bones consists of cortical bone. Cortical bone in the diaphysis can be characterized by measures of total area, marrow area and moment of inertias [3]. Total area is the area enclosed by the periosteum. Marrow area is the area enclosed by the endosteum. Moment of inertia is generally measured about the medial-lateral axis and anterior-posterior anatomical axes (Fig. 1.2A), and their ratio describes the ellipticity of the cross section. Cortical area is a measure of bone mass accumulation. Trabecular bone has a complex microstructure that is most often defined by the bone volume fraction (BV/TV), although other measures of microstructure are also available (Fig 1.2B).

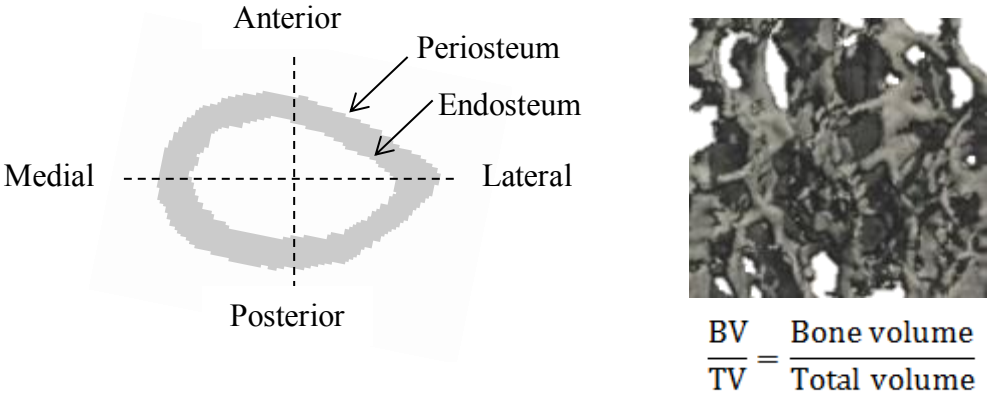

Figure 1.2: Examples of (A) cortical and (B) trabecular bone analyzed for bone morphology.

Bone tissue material properties are determined by the overall composition of bone and biophysical properties of the components [4]. The relative amounts of mineral, organic matrix (collagenous and non-collagenous proteins) and water influence bone tissue material properties. The size and shape of the mineral crystals and the type and degree of cross-linking of collagen fibrils are biophysical properties that are associated with whole bone mechanical properties [4].

1.3 Bone Growth and Development

The majority of our bones are generated during growth (ages 0-16 years). Bone growth involves increases in size, increases in degree of mineralization and changes to bone external and internal morphology [5]. Longitudinal bone growth occurs at the growth plates through a well described process known as endochondral ossification. Endochondral ossification occurs through a process of cartilage synthesis and subsequent replacement of cartilage by bone (Fig. 1.3A). Changes in cross sectional geometry occur as a result of intramembranous ossification where bone is formed on the periosteum and is resorbed on the endosteum (Fig. 1.3B).

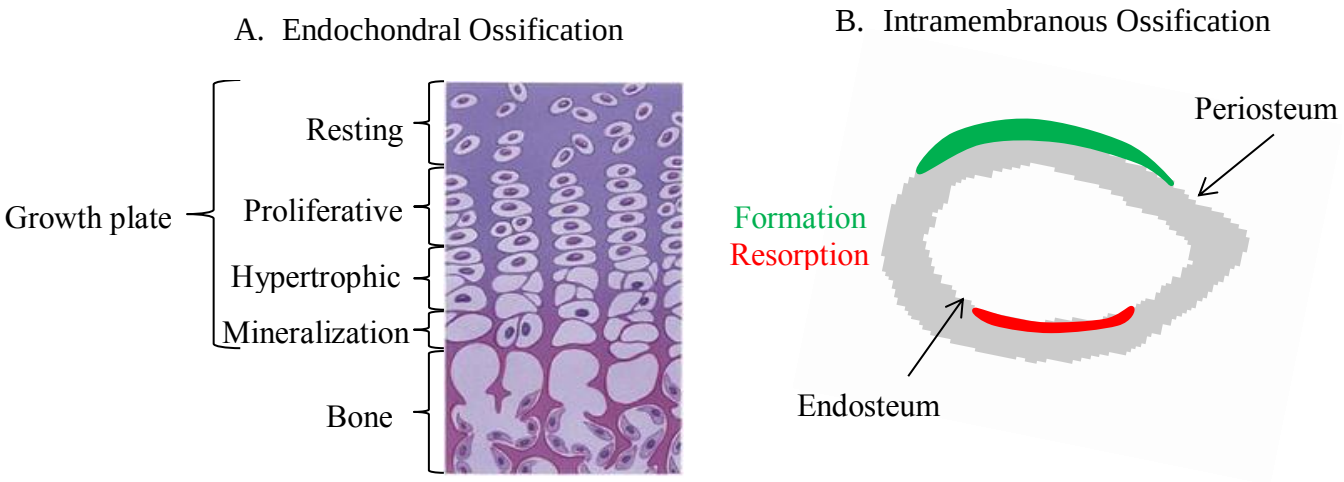

Figure 1.4: Depiction of the two types of bone growth is shown. (A) Endochondral ossification is shown where cartilage cells divide and grow before being replaced with bone tissue increasing the length of the bone, and (B) Intramembranous ossification is shown where bone is formed on already existing bone and bone is resorbed.

Even after skeletal maturity is reached, bone is not a static organ. Bone remodeling is constantly altering bone shape. Bone remodeling is an orchestrated process of bone resorption and subsequent bone formation in the same location [6]. Newly formed bone undergoes a mineralization process and reaches 70% of its total mineralization a few days after being formed.

1.4 Understanding Fracture Risk

We are interested in understanding the causes of fracture risk. We can mimic human disease in animals using surgeries, alterations to the diet or by looking at genetic models. To determine how an experimental perturbation affects bone phenotype, we look at changes to bone morphology and mechanical performance.

1.4.1 Mechanical Properties of Cortical Bone

Cortical bone in the diaphysis is commonly evaluated in mouse models of bone disease. Although bone morphology can be determined using histology and gross measurements, microcomputed tomography (μCT) is the current standard for assessing bone structure in mice. Images of the mouse bone collected with μCT are submitted to image processing steps to separate the mineralized bone tissue from background and quantify bone mass and distribution.

Common morphological parameters analyzed include bone length, total area, marrow area, cortical area and moment of inertia. A region representing 2.5% of the bone length centered halfway along the length of the bone is used to analyze cross-sectional geometry associated with whole bone bending [7].

The small size of mouse bones makes examining machined specimens of controlled shape challenging. For this reason, the most common biomechanical assessment of mouse bone is bending tests applied to a long bone, most often the femur (Fig.1.4).

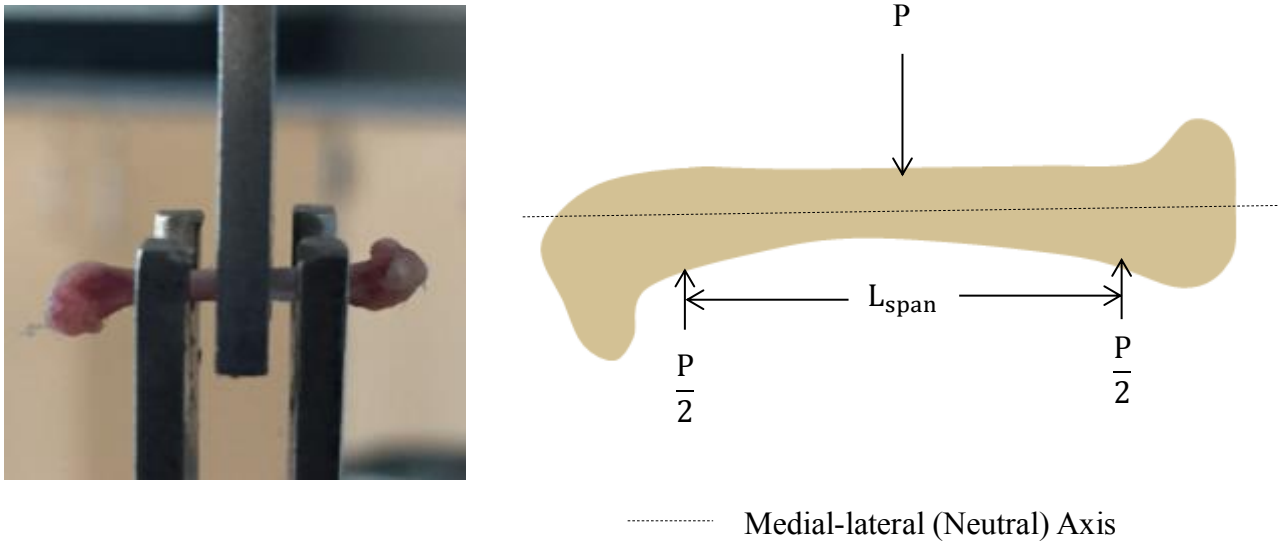

Figure 1.5: Femurs tested in three-point bending to determine mechanical properties. Top crosshead loads the bone at a rate of 0.1 mm/s until failure. The corresponding free body diagram is shown.

Whole bone mechanical properties of interest are peak load, stiffness and post yield displacement. A regression line with a slope representative of a 10% loss in stiffness starting at the beginning of the linear region intersects with the load-displacement curve at the yield point.

Peak moment (M_{max}) relates to tissue material strength in bending (σ_b) by the following equation (Eq. 1.1):

$$M_{max} = \sigma_b * \frac{I}{c} \quad (1.1)$$

for which $\frac{I}{c}$ are the key geometric parameters relating applied load to tissue stress. To avoid making assumptions about femur geometry, we can plot peak moment against $\frac{I}{c}$ and differences in regression lines can be attributed to an effect of the perturbation on tissue material properties.

1.4.2 Mechanical Properties of Cancellous Bone

Cancellous bone has a more complex microstructure than cortical bone and is challenging to evaluate mechanically. Methods of mechanically testing cancellous bone that provide boundary conditions to reduce systemic and random errors in compression tests were established in the 1990s [8]. The method involves press fitting cancellous bone cores into brass endcaps (Loctite 406 Prism Instant Adhesive, Applied Industrial Technologies, MA4230111). An extensometer is attached to the endcaps to measure displacement (Fig. 1.5). The specimen is loaded in displacement control.

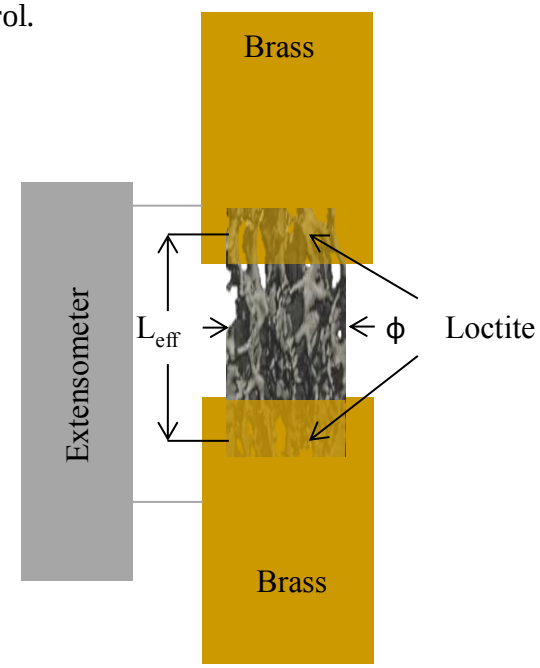

Figure 1.6: Cancellous cores tested in compression for which the sample is first preconditioned to reduce hysteresis before load is ramped to a predetermined strain

Stress and strain are calculated from the load and displacement data using the diameter (ϕ) of the core and the effective length (L_{eff}). L_{eff} is calculated as the exposed length plus half the length in the endcaps. The results of interest are Young's modulus, yield stress and strain, ultimate stress and strain and toughness. The yield point is determined using the 0.2% offset method. Bone volume fraction and tissue material properties influence these structural properties in monotonic compression loading.

1.5 Obesity and Bone

Obesity has traditionally thought to be beneficial for bone health as heavier individuals apply greater loads to their bones, resulting in greater bone mass. However, obesity has been associated with increases in fracture risk that is not explained by associated changes in bone mineral density [9]. Animal models of obesity have been used to study the effect of obesity on bone mass and mechanical properties.

Animal models of obesity include high fat diet (HFD), leptin receptor deficient (db/db) and leptin deficient (ob/ob) mice. The HFD mouse bone phenotype is characterized by reduced trabecular bone mass and impaired cortical bone tissue material properties [10, 11]. There has been conflicting results of the effect of leptin deficiency and leptin receptor deficiency on bone mass [12, 13]. These animal models exhibit severe obesity that can lead to symptoms of type 2 diabetes. Animal models of obesity do not mimic more common levels of obesity seen in humans.

1.6 Osteoporosis and PTH Therapy

Osteoporosis is a metabolic bone disease characterized by severe bone loss and is diagnosed by a low BMD score compared to that of a healthy 30 year-old. Osteoporosis is associated with increased risk of fragility fracture. Drug treatments are used to reverse the bone loss and reduce fracture risk in people with osteoporosis. Pharmaceuticals used to treat

osteoporosis are classified as either anti-resorptive or anabolic. Anti-resorptive drugs work by decreasing rates of bone resorption resulting in decreased bone remodeling and increased BMD. Anabolic agents work by increasing bone formation. Both classes of drugs have been shown to decrease fracture risk in osteoporotic patients [14, 15].

Parathyroid hormone (PTH) is an example of an anabolic agent used to treat osteoporosis. PTH therapy works by increasing bone formation by stimulating bone remodeling [16]. Clinically and in small animal models PTH treatment increases bone mass and improve mechanical properties.

1.7 Objective

The objective of this thesis was to characterize the mechanical properties of cortical bone in a mouse model of metabolic syndrome and of cancellous bone in a sheep model of osteopenia. These two animal models mimic two populations of people for whom we are interested in understanding their risk of fragility fracture.

1.7.1 Aim 1

Obesity is a common precursor to metabolic syndrome [17]. The increased risk of fragility fracture associated with obesity may also be associated with metabolic syndrome. Metabolic syndrome is the presence of three or more of the following metabolic disorders: abdominal obesity, high triglycerides, low HDL-cholesterol, high blood pressure and high blood glucose [18]. Current animal models of obesity are not representative of the obesity levels associated with metabolic syndrome seen in humans. The toll-like receptor 5 deficient (TLR5KO) mouse displays metabolic syndrome with a more modest level of obesity and has been shown to have impaired cortical bone tissue material properties at 16 weeks in male mice [19]. The goal of this aim was to fully characterize the cortical bone phenotype of TLR5KO mice. Both male and female mice were used in this study and examined 10-55 weeks of age to

determine if age or sex modulated the effect of genotype. Changes to bone morphology and mechanical performance were assessed in the femoral mid-diaphysis by μCT and mechanical testing in three-point bending.

1.7.2 Aim 2

Osteoporosis affects an estimated 200 million people worldwide and 8.9 million osteoporotic fractures occur per year [20]. Parathyroid hormone (PTH) is a treatment for osteoporosis that increases bone formation by stimulating bone remodeling. The goal of this aim was to determine the effect of PTH treatment on mechanical properties of cancellous bone in compression in a sheep model of osteopenia. Osteopenia was induced in sheep (6-7 years old) via ovariectomy (OVX) and a diet to induce metabolic acidosis (MA). Osteopenia was developed over a year. The sheep were treated with either vehicle (n = 6) or PTH (n = 7) for a year. In this study, the monotonic mechanical properties of cancellous cores from the distal femur were determined.

REFERENCES

[1] K.E. Ensrud, Epidemiology of fracture risk with advancing age, J Gerontol A Biol Sci Med Sci 68(10) (2013) 1236-42.

[2] C.J. Hernandez, T.M. Keaveny, A biomechanical perspective on bone quality, Bone 39(6) (2006) 1173-81.

[3] K.J. Jepsen, M.J. Silva, D. Vashishth, X.E. Guo, M.C. van der Meulen, Establishing biomechanical mechanisms in mouse models: practical guidelines for systematically evaluating phenotypic changes in the diaphyses of long bones, J Bone Miner Res 30(6) (2015) 951-66.

[4] H. Fonseca, D. Moreira-Goncalves, H.J. Coriolano, J.A. Duarte, Bone quality: the determinants of bone strength and fragility, Sports Med 44(1) (2014) 37-53.

[5] V.L. Ferguson, R.A. Ayers, T.A. Bateman, S.J. Simske, Bone development and age-related bone loss in male C57BL/6J mice, Bone 33(3) (2003) 387-98.

[6] B. Clarke, Normal bone anatomy and physiology, Clin J Am Soc Nephrol 3 Suppl 3 (2008) S131-9.

[7] M.L. Bouxsein, S.K. Boyd, B.A. Christiansen, R.E. Guldberg, K.J. Jepsen, R. Muller, Guidelines for Assessment of Bone Microstructure in Rodents Using Micro-Computed Tomography, Journal of Bone and Mineral Research 25(7) (2010) 1468-1486.

[8] T.M. Keaveny, T.P. Pinilla, R.P. Crawford, D.L. Kopperdahl, A. Lou, Systematic and random errors in compression testing of trabecular bone, J Orthop Res 15(1) (1997) 101-10.

[9] H. Johansson, J.A. Kanis, A. Oden, E. McCloskey, R.D. Chapurlat, C. Christiansen, S.R. Cummings, A. Diez-Perez, J.A. Eisman, S. Fujiwara, C.C. Gluer, D. Goltzman, D. Hans, K.T. Khaw, M.A. Krieg, H. Kroger, A.Z. LaCroix, E. Lau, W.D. Leslie, D. Mellstrom, L.J. Melton, 3rd, T.W. O'Neill, J.A. Pasco, J.C. Prior, D.M. Reid, F. Rivadeneira, T. van Staa, N. Yoshimura, M.C. Zillikens, A meta-analysis of the association of fracture risk and body mass index in women, J Bone Miner Res 29(1) (2014) 223-33.

[10] J.A. Inzana, M. Kung, L. Shu, D. Hamada, L.P. Xing, M.J. Zuscik, H.A. Awad, R.A. Mooney, Immature mice are more susceptible to the detrimental effects of high fat diet on cancellous bone in the distal femur, Bone 57(1) (2013) 174-83.

[11] S.S. Ionova-Martin, S.H. Do, H.D. Barth, M. Szadkowska, A.E. Porter, J.W. Ager, 3rd, J.W. Ager, Jr., T. Alliston, C. Vaisse, R.O. Ritchie, Reduced size-independent mechanical properties of cortical bone in high-fat diet-induced obesity, Bone 46(1) (2010) 217-25.

[12] P. Ducy, M. Amling, S. Takeda, M. Priemel, A.F. Schilling, F.T. Beil, J.H. Shen, C. Vinson, J.M. Rueger, G. Karsenty, Leptin inhibits bone formation through a hypothalamic relay: A central control of bone mass, Cell 100(2) (2000) 197-207.

[13] M.W. Hamrick, C. Pennington, D. Newton, D. Xie, C. Isales, Leptin deficiency produces contrasting phenotypes in bones of the limb and spine, Bone 34(3) (2004) 376-383.

[14] J.P. Bilezikian, Efficacy of bisphosphonates in reducing fracture risk in postmenopausal osteoporosis, Am J Med 122(2 Suppl) (2009) S14-21.

[15] R.M. Neer, C.D. Arnaud, J.R. Zanchetta, R. Prince, G.A. Gaich, J.Y. Reginster, A.B. Hodsman, E.F. Eriksen, S. Ish-Shalom, H.K. Genant, O. Wang, B.H. Mitlak, Effect of

parathyroid hormone (1-34) on fractures and bone mineral density in postmenopausal women with osteoporosis, N Engl J Med 344(19) (2001) 1434-41.

[16] E. Canalis, A. Giustina, J.P. Bilezikian, Mechanisms of anabolic therapies for osteoporosis, New Engl J Med 357(9) (2007) 905-916.

[17] S.M. Grundy, Obesity, metabolic syndrome, and cardiovascular disease, J Clin Endocr Metab 89(6) (2004) 2595-2600.

[18] M. Aguilar, T. Bhuket, S. Torres, B. Liu, R.J. Wong, Prevalence of the metabolic syndrome in the United States, 2003-2012, JAMA 313(19) (2015) 1973-4.

[19] J.D. Guss, M.W. Horsfield, F.F. Fontenele, T.N. Sandoval, M. Luna, F. Apoorva, S.F. Lima, R.C. Bicalho, A. Singh, R.E. Ley, M.C. van der Meulen, S.R. Goldring, C.J. Hernandez, Alterations to the Gut Microbiome Impair Bone Strength and Tissue Material Properties, J Bone Miner Res 32(6) (2017) 1343-1353.

[20] P. Pisani, M.D. Renna, F. Conversano, E. Casciaro, M. Di Paola, E. Quarta, M. Muratore, S. Casciaro, Major osteoporotic fragility fractures: Risk factor updates and societal impact, World J Orthop 7(3) (2016) 171-81.

CHAPTER 2

BONE PHENOTYPE OF THE TOLL-LIKE RECEPTOR FIVE DEFICIENT MOUSE

2.1 Introduction

Nine million people worldwide experience a fragility fracture a year [1]. A bone fracture that results from a low-level trauma such as falling from standing height is defined as a fragility fracture. To assess a person's risk of a fragility fracture, bone mineral density (BMD) provides a snapshot of bone health. Low BMD is associated with an increased risk of fracture.

Obesity is associated with increased fragility fracture risk that is not explained by changes in BMD. Mouse models are useful for studying disease mechanisms and testing the feasibility of interventions. Mouse models of obesity that have been used to study bone include high fat diet (HFD), leptin deficient (ob/ob) and leptin receptor deficient (db/db). All three of these mouse models of obesity develop other metabolic abnormalities including insulin resistance, hyperglycemia and hypertension reminiscent of what is seen in humans [3, 4]. High fat diet induces trabecular bone loss [5, 6] and conflicting results on cortical bone mass [5, 7-8]. HFD results in impaired cortical bone tissue material properties [7, 8] and reduced degree of mineralization [9] compared to wild type (WT). Leptin deficient mice have been reported to have increased [10, 11] and decreased [12-14] bone mass in the appendicular skeleton compared to WT. In the axial skeleton, leptin deficient mice have been reported to have increased trabecular bone mass [10-14] (Table 2.1). The large increase in adiposity (136-200% of WT body mass) of obesity models is representative of severe obesity. However, a large number of patients that are overweight but do not have severe obesity are diagnosed with metabolic syndrome.

Metabolic syndrome (MetS) is a cluster of risk factors for cardiovascular disease (CVD) and type II diabetes (T2D) that include abdominal obesity, high triglycerides, reduced HDL-

cholesterol, high blood pressure and high fasting glucose. An estimated 34% of the U.S. adult population meets the criteria for metabolic syndrome [2].

Table 2.1: Mouse models of metabolic syndrome and bone phenotype are shown

Model	Traits of MetS	% Increase in Body Mass	Appendicular Skeleton	Axial Skeleton
TLR5KO [15, 18]	Mild obesity Insulin resistance High blood pressure High blood glucose	20%	↓ Peak moment adjusted for geometry ↑ Femoral total area and moment of inertia No effect on tibial cancellous bone mass No effect on TMD	-
HFD [5-9]	Obesity Insulin resistance High blood glucose Hypertension	30-55%	↓Cancellous bone mass No effect on cortical bone mass ↑ Cortical bone mass ↓ Femoral bone mineral density ↓Cortical bone material properties	↓ Cancellous bone mass ↓ Compressive max load ↓Bone mineral density
Leptin receptor deficient (db/db) [10, 11, 13, 14]	Obesity Insulin resistance High blood glucose	70%	↓ Trabecular bone volume fraction ↓Cortical bone mass ↑ Trabecular bone mass No effect on cortical bone ↓ Decreased femoral max load	↓Trabecular thickness ↑Trabecular bone mass
Leptin deficient (ob/ob) [10-12, 14]	Severe obesity Insulin resistance High blood glucose	>100%	↑Trabecular bone mass ↓ Femur length, cortical thickness, mineral content and density and trabecular bone volume	↑ Trabecular bone mass ↑ Length, mineral content and density and trabecular bone volume

The toll-like receptor 5 deficient (TLR5KO) mouse is congenic mouse strain that displays metabolic syndrome with levels of obesity less (20% greater body mass than wild type) than that of other commonly used models (30-100% greater body mass than wild type) [15]. Toll-like receptor 5 (TLR5) is an innate immune receptor that recognizes flagellin [16]. TLR5KO mice fail to respond to flagellin resulting in alterations to the gut microbiome that lead to systemic and intestinal inflammation and a metabolic syndrome-like state characterized by mild obesity, insulin resistance, increased blood pressure and increased blood glucose [15, 17].

Recently, TLR5KO mice were shown to have differences in bone mass and strength as compared to wild type controls [18]. Both the tibia and femur were analyzed in male mice at 16 weeks. TLR5KO mice had greater femoral cortical bone total area and moment of inertia about the medial-lateral axis, but no differences were observed in peak load, stiffness and post yield displacement between TLR5KO and WT mice. The increased bone geometry with no differences in peak moment indicated impaired tissue material properties. No differences in cancellous bone mass and tissue mineral density of the tibia were observed between TLR5KO and WT.

Sex [19] and age [20-22] are two factors known to influence bone mass and mechanical performance. Female mice bone size and mechanical properties are different than those of male mice even after adjusting for body size [19]. Bone size and material properties change rapidly until skeletal maturity is reached. Skeletal maturity is reached between 12 and 16 weeks in mice [21]. Differences in TLR5KO bone phenotype between male and female mice or during aging may indicate distinct mechanisms to explain the observed changes in bone mechanical performance.

The goal of the current study is to test the hypothesis that toll-like receptor 5 deficiency impairs cortical bone tissue material properties in both male and female mice. Specifically, we

determined femur structure and strength in male and female TLR5KO mice at ages 10-55 weeks and compared the bone phenotype to that of WT controls.

2.2 Material and Methods

Under approval of the local IACUC, C57BL/6J and B6.129S1-Tlr5tm1Flv/J (TLR5KO) mice were acquired from Jackson and bred separately. The TLR5KO mouse is a congenic strain that has been backcrossed to the C57BL/6J background. The C57BL/6J is an appropriate WT control for TLR5KO [15, 23]. Animal were housed in plastic cages filled with ¼-inch corn cob bedding (The Anderson' Lab Bedding, Ohio), provided a cardboard refuge environmental enrichment hut (Ketchum Manufacturing; Brockville, Ontario) and fed standard laboratory chow (Teklad LM-485 Mouse/Rat Sterilizable Diet) and water *ad libitum*. Female mice were euthanized at 10, 16 and 20 weeks of age and male mice were euthanized at 10, 16, 20 and 55 weeks of age (n = 5-19/group, 201 total) (Table 2.2). The 16 week male mice were described in a prior work [18]. Epididymal fat pad mass and femora were collected after euthanasia.

Table 2.2: Sample sizes are shown.

Age (wks)	10		16		20		55	
	WT	TLR5KO	WT	TLR5KO	WT	TLR5KO	WT	TLR5KO
Male	11	8	12	16	5	9	10	10
Female	13	7	8	19	9	19	-	-

2.2.1 Cortical bone mechanical testing

Right femora were harvested, wrapped in PBS soaked gauze and stored at -20°C prior to analysis. Femoral length was measured from the greater trochanter to the lateral condyle. Microcomputed tomography (μCT) images of the femoral diaphysis were obtained with a voxel size of 25 μm (GE eXplore CT 120; 80 kVp, 32 μA, 100 ms integration time). Images were

submitted to a Gaussian filter to remove noise, and a global threshold was used to segment mineralized bone from background. A region representing 2.5% of the femur length and centered midway between the greater trochanter and lateral condyle was used to determine femoral cross-sectional geometry (total area, cortical area, marrow area and moment of inertia about the medial-lateral axis). After imaging, samples were stored frozen at -20°C until mechanical testing.

Femora were thawed at room temperature prior to mechanical testing and kept hydrated during testing. Right femora were loaded in three point bending to failure at rate of 0.1 mm/s (858 Mini Bionix; MTS, Eden Prairie, MN, USA). Force was measured using a 100 lb load cell (Transducer Techniques, SSM-100, Temecula, CA), and displacement was measured using linear variable differential transducer at a 100 Hz sampling rate.

Stiffness was measured as the slope of the linear portion of the load displacement curve and adjusted for span length according to the following equation [24] (Eq. 2.1):

$$S = \left(\frac{P}{y}\right) * \frac{L^3}{48} \quad (2.1)$$

where S is the bending rigidity, $\frac{P}{y}$ is the unadjusted stiffness and L is the span length. Whole bone strength was evaluated as the maximum bending moment that could be applied to the bone. Peak bending moment was calculated as half the peak load times half the span length [24]. Femoral diaphyseal cross-sectional geometry and tissue material properties influence the peak moment as described by the following equation [25] (Eq. 2.2):

$$M = \sigma_b * \frac{I}{c} \quad (2.2)$$

where σ_b is the tissue material strength in bending, I is the moment of inertia and c is the distance from the neutral axis to the bone surface. The parameter $\frac{I}{c}$ represents the contribution of

cross-sectional geometry to peak moment. Differences in peak moment not explained by $\frac{I}{c}$ can be attributed to differences in tissue material properties.

2.2.2 Statistical Analyses

Comparisons of bone geometry among mouse strains are commonly performed after adjustment for body size [24]. In this cohort, there were only weak associations between bone geometry within each group. For this reason, we analyzed raw (unadjusted) measures of bone geometry. All statistics were run separately for male and female mice. To determine if mouse strain influenced a bone size or mechanical property, we performed an analysis of covariance (ANCOVA), implemented with a generalized linear model (GLM) (Eq. 2.3).

$$\text{Parameter} = \beta_0 + \beta_1 * \text{Age} + \beta_2 * \text{Genotype} + \beta_3 * \text{Age} * \text{Genotype} \quad (2.3)$$

The mean effect of genotype was calculated as $100 * \frac{\beta_2}{\beta_0}$. A significant cross term indicated an age dependent effect of genotype. A one-way ANOVA was performed to test for differences between mouse strains at each age. Homogenous variance was tested using Levene's test and normality tested using the Shapiro-Wilk test.

To determine if genotype affected whole bone bending strength in ways that were not explained by cross sectional geometry, we performed an ANCOVA, implemented with a GLM, with age and $\frac{I}{c}$ as covariates and genotype as a fixed effect. Statistics were computed using JMP Pro (v.12, 2016; SAS Institute Inc., Cary, NC, USA)

2.3 Results

2.3.1 TLR5KO genotype

Both male and female TLR5KO mice had increased body mass and epididymal fat pad mass compared to those of WT (Table 2.3). TLR5KO male mice had on average a 12.84% greater body mass and 93.89% greater epididymal fat pad mass than WT mice ($p < 0.05$,

determined from GLM coefficients, see Methods) (Fig. 2.1A-B). TLR5KO female mice had on average a 9.36% greater body mass and 88.60% greater epididymal fat pad mass than WT mice (Fig. 1.1C-D).

Table 2.3: Body mass and fat pad mass of mice shown (Mean ± SD)

	Age (wks)	10		16		20		55	
		WT	TLR5KO	WT	TLR5KO	WT	TLR5KO	WT	TLR5KO
Male	Body weight (g)	24.72 ± 1.54	26.76 ± 2.48	28.36 ± 1.03	31.30 ± 2.80	28.40 ± 1.93	30.07 ± 4.92	36.21± 2.67	49.21 ± 7.10
	Fat pad mass (g)	0.37 ± 0.056	0.43 ± 0.10	0.51 ± 0.11	0.77 ± 0.31	0.53 ± 0.13	0.92 ± 0.49	1.47 ± 0.41	2.53 ± 0.56
Female	Body weight (g)	19.31 ± 1.39	22.01 ± 1.24	22.35 ± 0.99	24.17 ± 3.86	21.24 ± 1.31	26.18 ± 4.37	-	-
	Fat pad mass (g)	0.21 ± 0.07	0.29 ± 0.11	0.21 ± 0.06	0.70 ± 0.53	0.27 ± 0.08	0.91 ± 0.56	-	-

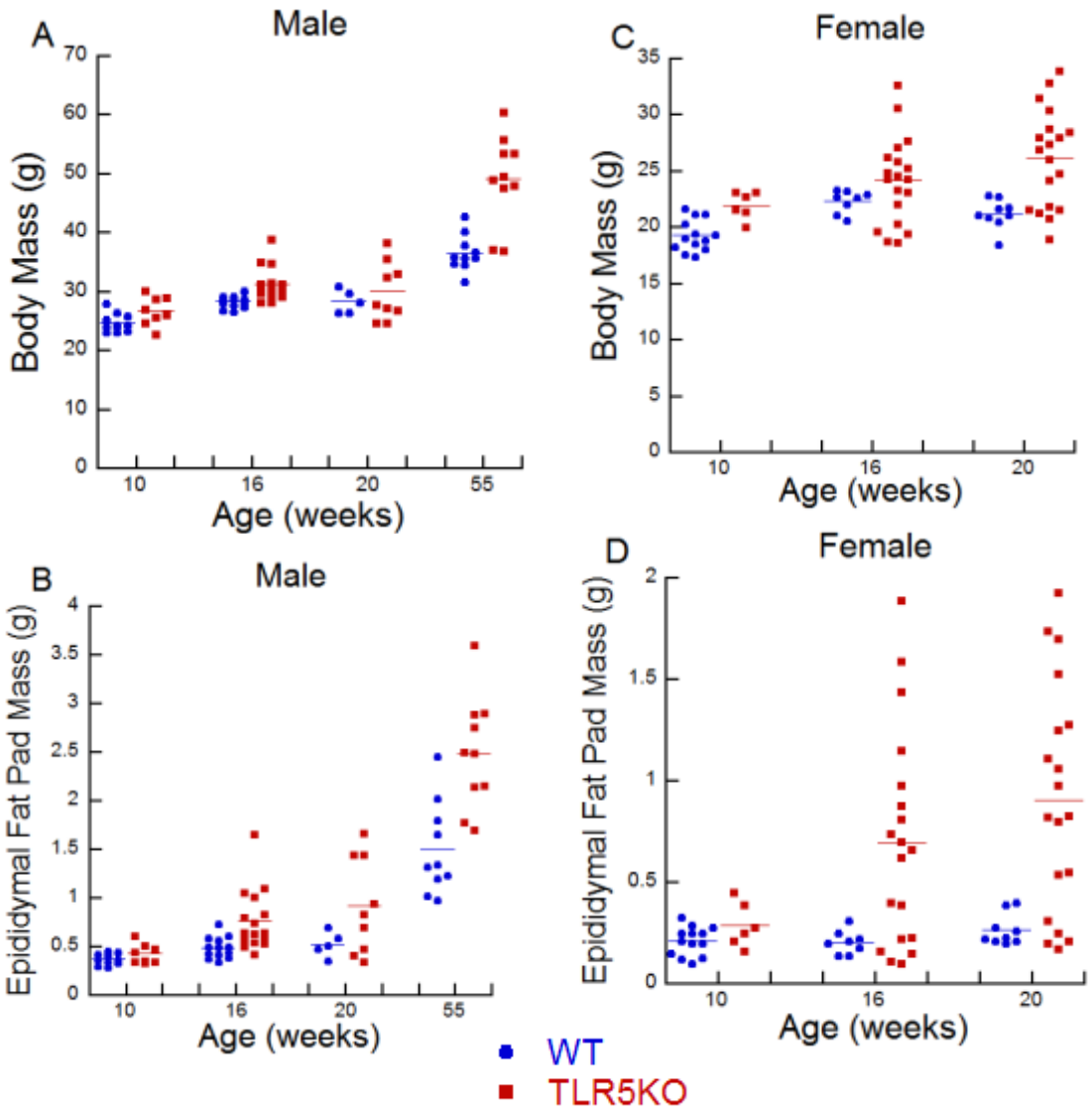

Figure 2.1: TLR5KO male and female mice had elevated body mass and fat pad mass compared to WT. (A) Body mass and (B) fat pad mass of male mice are shown. (C) Body mass and (D) fat pad mass of female mice are shown.

2.3.2 Whole bone mechanical performance

TLR5KO mice showed reduced whole bone bending strength after accounting for age and $\frac{I}{c}$ (Eq. 2.4). The effect of genotype was observed in both male and female mice (Table 4). The peak moment of bones from TLR5KO male mice were, on average, 10.09% less than WT after taking into account age and $\frac{I}{c}$ ($p < 0001{,}100^* \frac{\beta_3}{\beta_0}$ from Eqn. 2.4 below). The peak moment of

bones from TLR5KO female mice were, on average, 9.74% less than WT after taking into account age and $\frac{I}{c}$ ($p < 0.05$).

$$M_{max} = \beta_0 + \beta_1 * \frac{I}{c} + \beta_2 * \text{Age} + \beta_3 * \text{Genotype} + \beta_4 * \frac{I}{c} * \text{Age} + \beta_5 * \frac{I}{c} * \text{Genotype} \quad (2.4)$$

Table 2.4: Significant effects in multivariate linear regression of peak moment (Eq. 2.4) are shown.

	I/c	Age	Genotype	I/c*Age	I/c*Genotype
Peak moment (Male)	$p < 0.0001$	$p < 0.0001$	$p < 0.0001$	$p = 0.0063$	$p = 0.001$
Peak moment (Female)	$p < 0.0001$	$p < 0.0001$	$p < 0.05$	NS	NS

Differences in peak moment were also observed within each age group. The peak moment of bones from the TLR5KO male mice at 16 weeks was 10.70% less than that of WT after taking into account $\frac{I}{c}$. At 16 weeks, the peak moment of bones from the TLR5KO female mice was 9.49% less than that of WT after accounting for $\frac{I}{c}$ (Fig. 2.2). Reduced whole bone bending strength after taking account $\frac{I}{c}$ was seen at most ages (Table 2.5). Differences in peak moment after accounting for $\frac{I}{c}$ between WT and TLR5KO ranged from 9 to 21%.

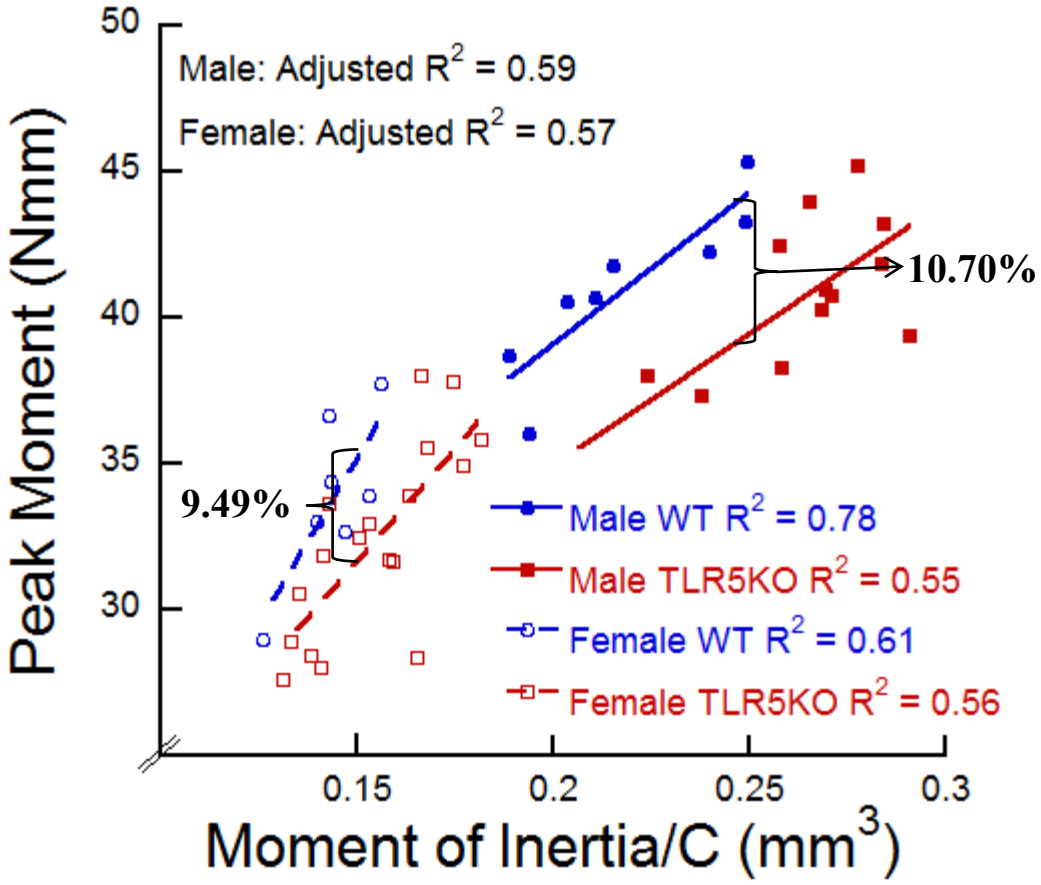

Figure 2.2: Whole bone bending strength is less in TLR5KO mice compared to that of WT after accounting for $\frac{I}{c}$ (visualized as the differences between blue and red lines). The effect of genotype was seen in both male (solid lines) and female mice (dashed lines).

Table 2.5: TLR5KO mice showed reduced mean peak bending moment after accounting for $\frac{I}{c}$ in most of the age groups. (Mean ± SD).

	Male			Female		
Age (wks)	WT	TLR5KO	% Difference	WT	TLR5KO	% Difference
10	38.54 ± 1.12	34.94* ± 0.93	-9.55	25.89 ± 1.17	22.11* ± 1.27	-13.96
16	43.56 ± 0.84	38.96* ± 0.61	-10.70	35.19 ± 0.85	31.85* ± 0.52	-9.49
20	38.98 ± 0.71	38.98 ± 0.71	0	36.71 ± 0.45	36.71 ± 0.45	0
55	35.71 ± 1.27	28.05* ± 1.27	-21.47	-	-	-

* different from WT ($p < 0.05$)

2.3.3 Femoral cross-sectional geometry

Genotype, on average, had no effect on total area in male or female mice (Fig. 2.3). TLR5KO male mice had, on average, 3.47% greater marrow area compared to WT ($p < 0.05$, determined from GLM coefficients, see Methods). Genotype was not associated with differences in cortical area in male mice. There were no differences in marrow area between TLR5KO and WT female mice. TLR5KO female mice had, on average, a 3.11% greater cortical area than WT ($p < 0.05$). Moment of inertia about the medial-lateral axis of TLR5KO female mice was on average 3.97% greater than WT ($p < 0.05$) (Fig. 2.4B). Moment of inertia, on average, was not different between TLR5KO and WT male mice (Fig. 2.4A). There was no effect of genotype on femur length in male or female mice.

The effect of genotype on cross-sectional geometry depended on the age and sex of the mice (Table 2.6). Total area of male TLR5KO mice at 16 weeks was greater than that of WT. Marrow area and cortical area were not different between TLR5KO and WT after taking into account total area at 10, 16 and 20 weeks (Eqn. 2.5). At 55 weeks, there was an effect of genotype on marrow area and cortical area after taking into account total area ($p < 0.05$, $100 * \frac{\beta_2}{\beta_0}$ from Eqn. 2.5 below). Marrow area was on average 22.12% greater and there was an equal reduction in cortical area of TLR5KO male mice at 55 weeks compared to WT after taking into account total area.

$$\text{Marrow or Cortical Area} = \beta_0 + \beta_1 * \text{Total Area} + \beta_2 * \text{Genotype} + \beta_3 * \text{Total Area} * \text{Genotype} \quad (2.5)$$

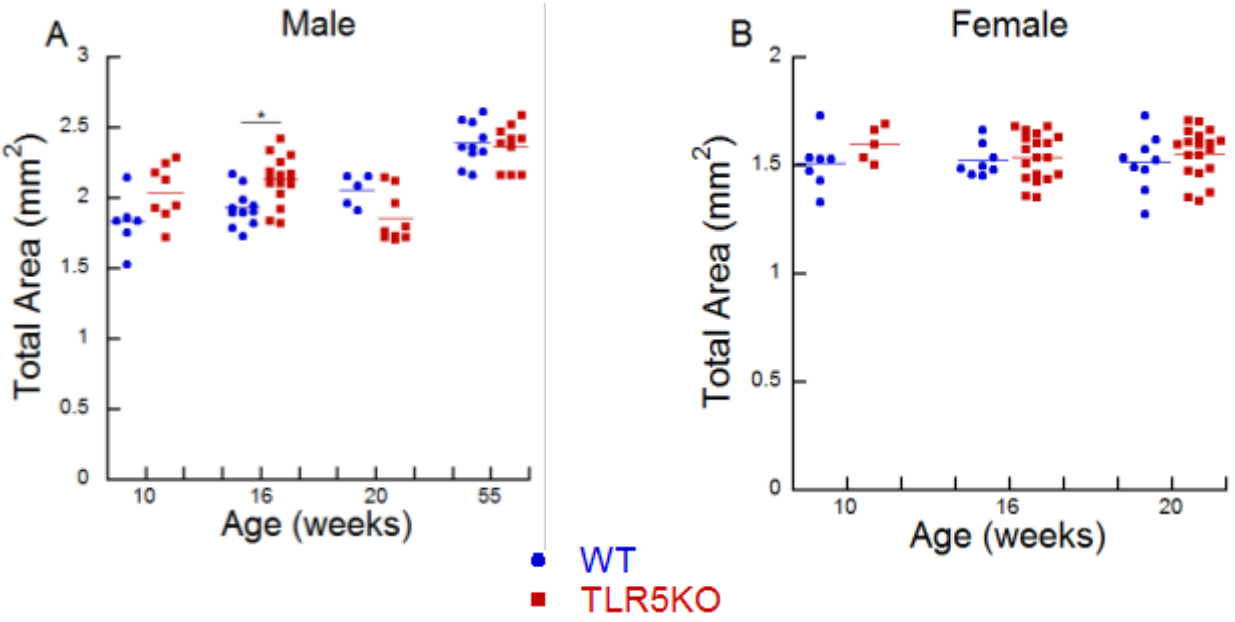

Figure 2.3: At 16 weeks of age, TLR5KO male mice have greater total area than that of WT. No differences in total area were observed between WT and TLR5KO at other ages in (A) male mice or (B) female mice.

Table 2.6: Femoral diaphyseal cortical bone morphology is shown. (Mean ± S.D).

	Age (wks)	10		16		20		55	
		WT	TLR5KO	WT	TLR5KO	WT	TLR5KO	WT	TLR5KO
Male	Femur length (mm)	15.47 ± 0.26	15.43 ± 0.22	16.05 ± 0.21	15.88 ± 0.26	15.82 ± 0.08	15.77 ± 0.34	16.10 ± 0.21	15.94 ± 0.33
	Total area (mm^2)	1.83 ± 0.20	2.05 ± 0.20	1.93 ± 0.13	2.13* ± 0.17	2.06 ± 0.11	1.86 ± 0.18	2.39 ± 0.15	2.37 ± 0.15
	Marrow area (mm^2)	1.05 ± 0.10	1.21 ± 0.10	1.06 ± 0.07	1.17* ± 0.15	1.18 ± 0.08	1.07 ± 0.10	1.40 ± 0.14	1.48 ± 0.12
	Cortical area (mm^2)	0.78 ± 0.14	0.83 ± 0.14	0.87 ± 0.07	0.96* ± 0.08	0.87 ± 0.05	0.79 ± 0.09	0.99 ± 0.11	0.89* ± 0.07
	Moment of Inertia (mm^4)	0.13 ± 0.03	0.16 ± 0.03	0.15 ± 0.02	0.18* ± 0.03	0.16 ± 0.03	0.13 ± 0.03	0.21 ± 0.03	0.19 ± 0.03
Female	Femur length (mm)	14.85 ± 0.38	15.07 ± 0.17	15.63 ± 0.13	15.46* ± 0.31	15.59 ± 0.60	15.72 ± 0.25	-	-
	Total area (mm^2)	1.51 ± 0.12	1.60 ± 0.079	1.53 ± 0.07	1.54 ± 0.11	1.52 ± 0.13	1.56 ± 0.11	-	-
	Marrow area (mm^2)	0.90 ± 0.06	0.94 ± 0.02	0.89 ± 0.08	0.88 ± 0.08	0.85 ± 0.06	0.85 ± 0.09	-	-
	Cortical area (mm^2)	0.61 ± 0.07	0.66 ± 0.08	0.63 ± 0.03	0.66 ± 0.06	0.66 ± 0.08	0.71 ± 0.05	-	-
	Moment of Inertia (mm^4)	0.09 ± 0.02	0.10 ± 0.01	0.09 ± 0.01	0.10 ± 0.01	0.09 ± 0.02	0.10 ± 0.01	-	-

* different from WT ($p < 0.05$)

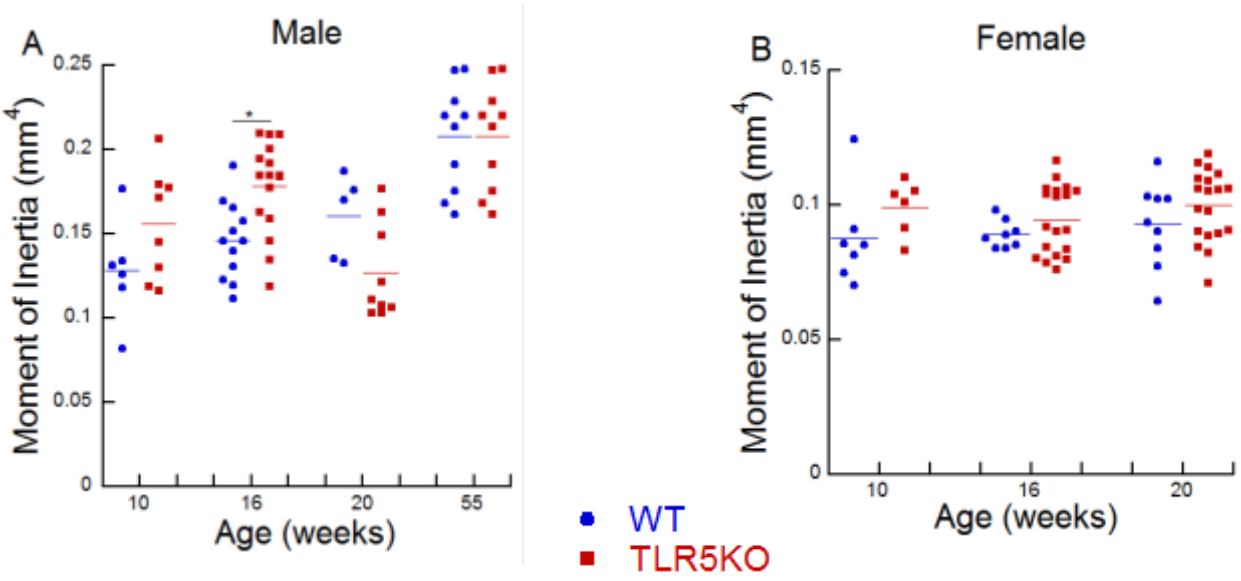

Figure 2.4: Moment of inertia is greater in TLR5KO male mice at 16 weeks compared to that of WT. No differences between WT and TLR5KO were observed in (A) male mice at 10, 20 or 55 weeks or in (B) female mice.

2.3.4 Mechanical performance

No effect of genotype on mechanical properties of female mice was observed. There was no effect of genotype, on average, on mechanical properties of male mice. In male TLR5KO mice, there were differences in mechanical properties at 20 and 55 weeks (Fig. 2.5). Peak moment of 55-week-old male TLR5KO mice was less than that of WT. Bending rigidity was reduced and post yield displacement was increased at 20 and 55 weeks in TLR5KO male mice compared to those of WT (Table 2.7).

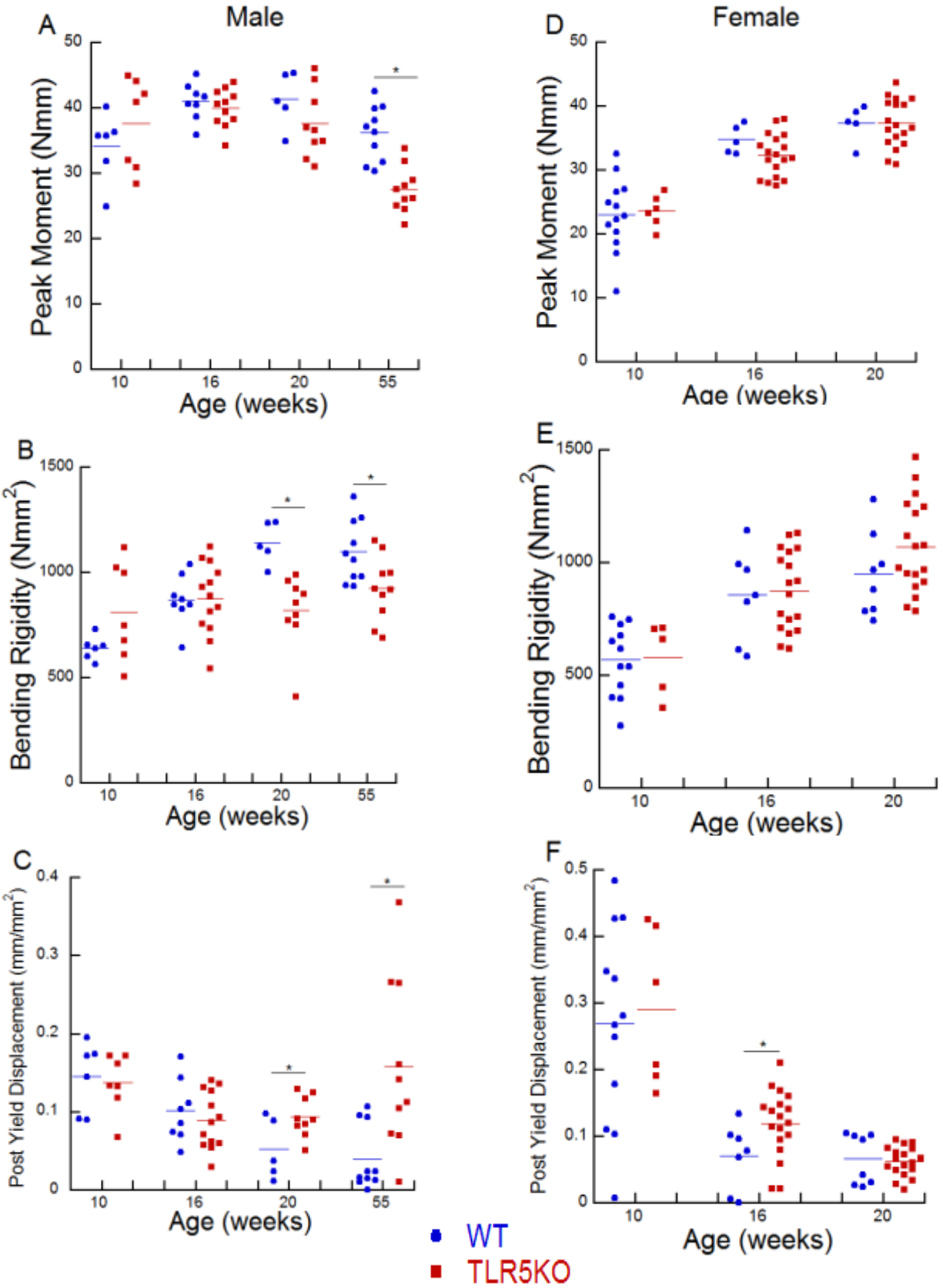

Figure 2.5: Mechanical properties of male (A-C) and female mice (D-F) are shown. (D-F) No differences were observed in peak moment, bending rigidity or post yield displacement between TLR5KO and WT female mice. (A) Peak moment was reduced in TLR5KO male mice at 55 weeks of age compared to that of WT. (B, C) Bending rigidity was reduced and post yield displacement was increased in TLR5KO male mice at 20 and 55 weeks of age compared to those of WT. No differences in peak moment, bending rigidity or post yield displacement were observed between TLR5KO and WT in male mice at 10 or 16 weeks of age.

Table 2.7: Differences between TLR5KO and WT in mechanical properties only at 20 and 55 weeks in male mice. (Mean ± S.D).

	Age (wks)	10		16		20		55	
		WT	TLR5KO	WT	TLR5KO	WT	TLR5KO	WT	TLR5KO
Male	Peak moment (Nmm)	34.23 ± 5.24	37.70 ± 6.94	41.09 ± 2.84	40.47 ± 3.00	41.38 ± 4.27	37.68 ± 5.20	36.24 ± 4.22	27.52 ± 3.48
	Bending rigidity (Nmm^2)	642.16 ± 56.37	813.40 ± 234.25	872.32 ± 119.21	877.06 ± 170.39	1142.65 ± 99.85	819.96* ± 174.25	1100.93 ± 148.50	924.76* ± 152.91
	PYD (mm/mm^2)	0.15 ± 0.05	0.14 ± 0.04	0.10 ± 0.040	0.09 ± 0.04	0.05 ± 0.04	0.094* ± 0.026	0.041 ± 0.041	0.16* ± 0.11
Female	Peak moment (Nmm)	23.13 ± 5.66	23.66 ± 2.49	33.91 ± 2.85	32.35 ± 3.29	35.25 ± 4.63	37.36 ± 3.75	-	-
	Bending rigidity (Nmm^2)	569.03 ± 157.11	578.39 ± 163.01	858.22 ± 203.63	876.65 ± 175.59	949.65 ± 185.90	1070.77 ± 204.04	-	-
	PYD (mm/mm^2)	0.27 ± 0.15	0.29 ± 0.12	0.07 ± 0.05	0.12* ± 0.05	0.07 ± 0.04	0.06 ± 0.02	-	-

* different from WT ($p < 0.05$)

2.4 Discussion

In this study, we investigated the effects of metabolic syndrome on bone mechanical performance in male and female mice at multiple age points. The TLR5KO bone phenotype is characterized by differences in bending strength that are not explained by geometry, suggesting impaired cortical bone tissue material properties compared to those of WT. Evidence of impaired cortical bone tissue material properties in TLR5KO mice compared to those of WT was detected in male and female mice. Cross-sectional geometry and tissue material properties determine whole bone bending strength.

The geometric parameter $\frac{I}{c}$ describes the geometric contribution to whole bone bending strength. As expected, there was a significant positive correlation between peak moment and $\frac{I}{c}$

across all groups. However, $\frac{I}{c}$ alone did not explain the differences between genotypes at 10, 16 and 55 weeks suggesting that TLR5KO mice have impaired bone tissue material properties. While differences in whole bone bending strength after taking into account cross-sectional geometry was detected at 10, 16 and 55 weeks, no differences were observed in 20 week mice. We attribute the lack of effect at 20 weeks to random chance.

Changes in bone geometry of TLR5KO mice compared to those of WT between 10 and 20 weeks of age may be a mechanism employed by the skeleton to maintain whole bone bending strength despite impaired tissue material properties. Differences in bone geometry between TLR5KO and WT mice were dependent on the age and sex of the mice. At 55 weeks of age, TLR5KO male mice had reduced whole bone bending strength. There was reduced bone mass accumulation due to increased bone resorption on the inner surface than what would have been expected given the total area in TLR5KO male mice compared to that of WT.

While there are many mechanisms for changing bone volume, only a few methods of changing bone tissue material properties in a mechanically relevant manner are known: alterations in tissue degree of mineralization, alterations in collagen cross-linking or collagen content, alterations in non-collagenous proteins and matrix bound water content. The degree of mineralization did not differ between the two mouse strains at 16 weeks of age in either female mice (ash fraction, data not shown) or male mice (TMD, measured with μCT) [18]. Other factors such as collagen and non-collagenous proteins may help explain the decreased whole bone strength after taking into account cross-sectional geometry in TLR5KO mice.

We did not observe differences in trabecular BV/TV of the tibial metaphysis between the TLR5KO and WT male mice at 16 weeks [18]. There were no differences in trabecular bone

mass between mouse strains in female mice (L5 vertebra, data not shown) or male mice (tibial metaphysis) [18].

Our findings in the TLR5 deficient mouse suggest that alterations in the gut microbiota can lead to changes in bone tissue material properties. Toll-like receptor 5 is the innate immune receptor for flagellin and does not have an endogenous ligand [17]. Hence, the phenotype of the TLR5KO mouse is caused primarily by alterations in host-microbe interactions. The TLR5KO phenotype does not develop in germ free mice (mice raised in absence of live bacteria) [15] and can be prevented by chronic antibiotics [18]. Additionally, the phenotype can be transferred to mice by transfer of the gut microbiota [15]. The gut microbiome may be directly or indirectly influencing the bone phenotype [26]. In the TLR5KO mouse, it is not clear if the associated alterations to the gut microbiome directly influence bone mechanical performance or if the microbiome induced metabolic-like syndrome causes the changes seen in bone mechanical performance.

There are a number of strengths of the current study. First, the TLR5KO mice exhibit metabolic syndrome with only mild obesity (108% - 135% of WT body mass) compared to other available obesity models (130% - 200% of WT body mass). Another strength of the current study is the examination of the relationship between bending strength and cross-sectional geometry. A majority of prior studies of mouse bone either report only whole bone mechanical properties (without addressing the role of geometry) or calculates tissue material properties using beam theory. The current approach not only accounts for geometry when comparing bone strength among mice but also does not require assumptions regarding beam theory. Secondly, we studied both male and female mice with an age range of 10 to 55 weeks old. Sex and age are two factors that are known to influence bone phenotype.

There are some limitations that have to be considered. The current study is limited by not directly analyzing tissue material properties. Direct measures of tissue material properties could better explain the differences in mechanical performance; however, methods of assessing bone tissue material properties have their own limitations (see Supporting Information in Jepsen et. al. [24]). Secondly, the current study uses the C57BL/6J mice as control for the TLR5KO strain despite minor remnants of B6.129S1 strain. The TLR5KO congenic strain is backcrossed for 11 generation of C57BL/6J to ensure 99.9% identical genetics to minimize the potential effects of B6.129S1.

Despite these limitations, the observation that metabolic syndrome associated with alterations to the gut microbiome can affect whole bone bending in ways that are not explained by cross-sectional geometry suggests that the microbiome and metabolic syndrome can alter bone tissue material properties. Bone tissue material properties are a recognized contributor to "bone quality" [27]. Bone quantity and quality determine risk of fracture [28]. At 10, 16 and 20 weeks of age, changes in bone geometry maintained whole bone bending strength compared to that of WT despite impaired tissue material properties. However, at 55 weeks of age where bone mass accumulation due to increases in endosteal resorption was reduced in the TLR5KO mice compared to that of WT, whole bone mechanical properties were impaired. Changes in whole bone mechanical properties are often cited as a contributor of fracture risk that exceeds what is expected from BMD. Our findings in mice suggest that metabolic syndrome may contribute to the risk of fracture by impairing cortical bone tissue material properties.

REFERENCES

[1] K.E. Ensrud, Epidemiology of fracture risk with advancing age, J Gerontol A Biol Sci Med Sci 68(10) (2013) 1236-42.

[2] M. Aguilar, T. Bhuket, S. Torres, B. Liu, R.J. Wong, Prevalence of the metabolic syndrome in the United States, 2003-2012, JAMA 313(19) (2015) 1973-4.

[3] A.J. Kennedy, K.L. Ellacott, V.L. King, A.H. Hasty, Mouse models of the metabolic syndrome, Dis Model Mech 3(3-4) (2010) 156-66.

[4] S. Collins, T.L. Martin, R.S. Surwit, J. Robidoux, Genetic vulnerability to diet-induced obesity in the C57BL/6J mouse: physiological and molecular characteristics, Physiol Behav 81(2) (2004) 243-8.

[5] J.J. Cao, B.R. Gregoire, H.W. Gao, High-fat diet decreases cancellous bone mass but has no effect on cortical bone mass in the tibia in mice, Bone 44(6) (2009) 1097-1104.

[6] J.A. Inzana, M. Kung, L. Shu, D. Hamada, L.P. Xing, M.J. Zuscik, H.A. Awad, R.A. Mooney, Immature mice are more susceptible to the detrimental effects of high fat diet on cancellous bone in the distal femur, Bone 57(1) (2013) 174-83.

[7] S.S. Ionova-Martin, S.H. Do, H.D. Barth, M. Szadkowska, A.E. Porter, J.W. Ager, 3rd, J.W. Ager, Jr., T. Alliston, C. Vaisse, R.O. Ritchie, Reduced size-independent mechanical properties of cortical bone in high-fat diet-induced obesity, Bone 46(1) (2010) 217-25.

[8] S.S. Ionova-Martin, J.M. Wade, S. Tang, M. Shahnazari, J.W. Ager, N.E. Lane, W. Yao, T. Alliston, C. Vaisse, R.O. Ritchie, Changes in cortical bone response to high-fat diet from adolescence to adulthood in mice, Osteoporosis Int 22(8) (2011) 2283-2293.

[9] F. Parhami, Y. Tintut, W.G. Beamer, N. Gharavi, W. Goodman, L.L. Demer, Atherogenic high-fat diet reduces bone mineralization in mice, Journal of Bone and Mineral Research 16(1) (2001) 182-188.

[10] P. Ducy, M. Amling, S. Takeda, M. Priemel, A.F. Schilling, F.T. Beil, J.H. Shen, C. Vinson, J.M. Rueger, G. Karsenty, Leptin inhibits bone formation through a hypothalamic relay: A central control of bone mass, Cell 100(2) (2000) 197-207.

[11] M. Amling, S. Takeda, G. Karsenty, A neuro (endo)crine regulation of bone remodeling, Bioessays 22(11) (2000) 970-975.

[12] M.W. Hamrick, C. Pennington, D. Newton, D. Xie, C. Isales, Leptin deficiency produces contrasting phenotypes in bones of the limb and spine, Bone 34(3) (2004) 376-383.

[13] G.A. Williams, K.E. Callon, M. Watson, J.L. Costa, Y. Ding, M. Dickinson, Y. Wang, D. Naot, I.R. Reid, J. Cornish, Skeletal phenotype of the leptin receptor-deficient db/db mouse, J Bone Miner Res 26(8) (2011) 1698-709.

[14] C.M. Steppan, D.T. Crawford, K.L. Chidsey-Frink, H.Z. Ke, A.G. Swick, Leptin is a potent stimulator of bone growth in ob/ob mice, Regul Peptides 92(1-3) (2000) 73-78.

[15] M. Vijay-Kumar, J.D. Aitken, F.A. Carvalho, T.C. Cullender, S. Mwangi, S. Srinivasan, S.V. Sitaraman, R. Knight, R.E. Ley, A.T. Gewirtz, Metabolic Syndrome and Altered Gut Microbiota in Mice Lacking Toll-Like Receptor 5, Science 328(5975) (2010) 228-231.

[16] F. Hayashi, K.D. Smith, A. Ozinsky, T.R. Hawn, E.C. Yi, D.R. Goodlett, J.K. Eng, S. Akira, D.M. Underhill, A. Aderem, The innate immune response to bacterial flagellin is mediated by Toll-like receptor 5, Nature 410(6832) (2001) 1099-1103.

[17] T.C. Cullender, B. Chassaing, A. Janzon, K. Kumar, C.E. Muller, J.J. Werner, L.T. Angenent, M.E. Bell, A.G. Hay, D.A. Peterson, J. Walter, M. Vijay-Kumar, A.T. Gewirtz, R.E. Ley, Innate and Adaptive Immunity Interact to Quench Microbiome Flagellar Motility in the Gut, Cell Host Microbe 14(5) (2013) 571-581.

[18] J.D. Guss, M.W. Horsfield, F.F. Fontenele, T.N. Sandoval, M. Luna, F. Apoorva, S.F. Lima, R.C. Bicalho, A. Singh, R.E. Ley, M.C. van der Meulen, S.R. Goldring, C.J. Hernandez,

Alterations to the Gut Microbiome Impair Bone Strength and Tissue Material Properties, J Bone Miner Res 32(6) (2017) 1343-1353.

[19] K.J. Jepsen, E.M.R. Bigelow, S.H. Schlecht, Women Build Long Bones With Less Cortical Mass Relative to Body Size and Bone Size Compared With Men, Clin Orthop Relat R 473(8) (2015) 2530-2539.

[20] M.D. Brodt, C.B. Ellis, M.J. Silva, Growing C57Bl/6 mice increase whole bone mechanical properties by increasing geometric and material properties, J Bone Miner Res 14(12) (1999) 2159-66.

[21] C. Price, B.C. Herman, T. Lufkin, H.M. Goldman, K.J. Jepsen, Genetic variation in bone growth patterns defines adult mouse bone fragility, J Bone Miner Res 20(11) (2005) 1983-91.

[22] V.L. Ferguson, R.A. Ayers, T.A. Bateman, S.J. Simske, Bone development and age-related bone loss in male C57BL/6J mice, Bone 33(3) (2003) 387-98.

[23] M. Vijay-Kumar, C.J. Sanders, R.T. Taylor, A. Kumar, J.D. Aitken, S.V. Sitaraman, A.S. Neish, S. Uematsu, S. Akira, I.R. Williams, A.T. Gewirtz, Deletion of TLR5 results in spontaneous colitis in mice, J Clin Invest 117(12) (2007) 3909-21.

[24] K.J. Jepsen, M.J. Silva, D. Vashishth, X.E. Guo, M.C. van der Meulen, Establishing biomechanical mechanisms in mouse models: practical guidelines for systematically evaluating phenotypic changes in the diaphyses of long bones, J Bone Miner Res 30(6) (2015) 951-66.

[25] C.H. Turner, D.B. Burr, Basic biomechanical measurements of bone: a tutorial, Bone 14(4) (1993) 595-608.

[26] C.J. Hernandez, J.D. Guss, M. Luna, S.R. Goldring, Links Between the Microbiome and Bone, Journal of Bone and Mineral Research 31(9) (2016) 1638-1646.

[27] H. Fonseca, D. Moreira-Goncalves, H.J. Coriolano, J.A. Duarte, Bone quality: the determinants of bone strength and fragility, Sports Med 44(1) (2014) 37-53.

[28] C.J. Hernandez, T.M. Keaveny, A biomechanical perspective on bone quality, Bone 39(6) (2006) 1173-81.

CHAPTER 3

EFFECT OF PTH-TREATMENT ON MECHANICAL PROPERTIES OF CANCELLOUS BONE

3.1 Introduction

Osteoporosis-related fractures are a significant clinical concern with 8.9 million people experiencing an osteoporotic fracture a year worldwide [1]. Anabolic agents can be used to treat osteoporosis by increasing bone formation. Parathyroid hormone (PTH) is an anabolic drug that is approved by the FDA to treat osteoporosis. Patients with osteoporosis treated with PTH experience 9-13% increase in bone mineral density (BMD) of the lumbar spine and 3-6 % increase in BMD of the hip. Risk of vertebral fractures is reduced by 65-69% and risk of non-vertebral fractures is reduced by 35-54% [2, 3].

Small animal model studies have shown that intermittent treatment with PTH increases bone mass [4-9] and improves bone mechanical properties [10-13]. Assessment of the effect of PTH treatment on mechanical properties has been limited to the femoral neck [11] and vertebra [10, 12-13]. Large animal studies are needed to understand the effect of PTH treatment on cancellous bone mechanical performance. Monotonic and fatigue loading are necessary to fully characterize the effect of PTH treatment on mechanical performance of cancellous bone. Here, we focused on monotonic loading in compression.

The goal of this study was to test the hypothesis that increased bone formation due to PTH treatment would improve mechanical performance of cancellous bone. Specifically, we mechanically tested cancellous bone specimens from the right distal femur monotonically in compression from osteopenic sheep treated with PTH or vehicle.

3.2 Materials and methods

A sheep model of osteopenia was used in this study. Sheep were ovariectomized (OVX) at 6-7 years old and were kept on a metabolic acidosis (MA) diet to induce osteopenia. A year after OVX, sheep were treated with either vehicle (n = 6) or PTH (n = 7) for a year. Following euthanasia, femurs were collected and stored at -20°C. Cylindrical cores were cut using a diamond-tipped coring tool with a diameter of 7.5 mm (Starlite, Lancaster, PA, USA).

3.2.1 Sample preparation

Cancellous bone cores were cut from the medial-caudal quadrant of the right distal femur aligned with the principal trabecular orientation and stored at -20°C. Specimens had an average height-to-diameter ratio of 2.43:1 (length: 17.90 ± 6.22 mm and diameter: 7.36 ± 0.06 mm). Marrow was removed from the ends of the cores using a low-pressure water jet. Cores were press-fit into brass endcaps (Loctite 406 Prism Instant Adhesive, Applied Industrial Technologies, MA4230111). Specimens were stored at 4°C overnight to allow the glue to set before testing.

3.2.2 Mechanical testing

Cancellous cores were loaded in compression. Specimens were brought to room temperature prior to testing. Load was measured using a 200 lb load cell (SSM-100, Transducer Techniques, Temecula, CA), and displacement was measured with a 25-mm gauge length extensometer attached to the brass endcaps. The cancellous cores were preconditioned for 10 cycles at 1.25 Hz from 0 to 0.2% strain, and then the load was ramped to 3% strain at 0.5% strain/sec (858 Mini Bionix; MTS, Eden Prairie, MN, USA).

Stress and strain were calculated from the load and displacement data. The mechanical properties of interest were Young's modulus, yield stress and strain, ultimate stress and strain and toughness to ultimate. The yield point was determined based on the 0.2% offset method.

3.2.3 Microcomputed Tomography

Microcomputed tomography (μCT) images of cancellous specimens from the distal femur were obtained with a voxel size of 25 μm. Images were submitted to a Gaussian filter, and a global threshold was used to segment mineralized bone from background. The images of cancellous bone were used to determine bone volume fraction (BV/TV).

3.3 Results

No differences in mechanical properties in compression were detected between vehicle treated and PTH treated samples (Table 3.1). However, cancellous bone from PTH treated animals showed a trend towards increased Young's modulus and yield and ultimate stress (Fig. 3.1). Yield and ultimate stress were correlated with Young's modulus ($p < 0.001$).

Table 3.1: Results of compression test. Mean ± SD.

	Control (n=5)	PTH (n=6)	p-value
Young's modulus (MPa)	662.6 ± 312	839.3 ± 374	0.21
Yield stress (MPa)	4.15 ±1.6	4.96 ± 2.1	0.24
Yield strain (%)	0.86 ± 0.2	0.80 ± 0.1	0.26
Ultimate stress (MPa)	5.38 ± 1.7	5.91 ± 1.9	0.32
Ultimate strain (%)	2.32 ± 0.86	1.75 ± 0.66	0.13
Total Toughness to Ult (kJ/m^3)	91.15 ± 44.0	70.24 ± 20.1	0.18

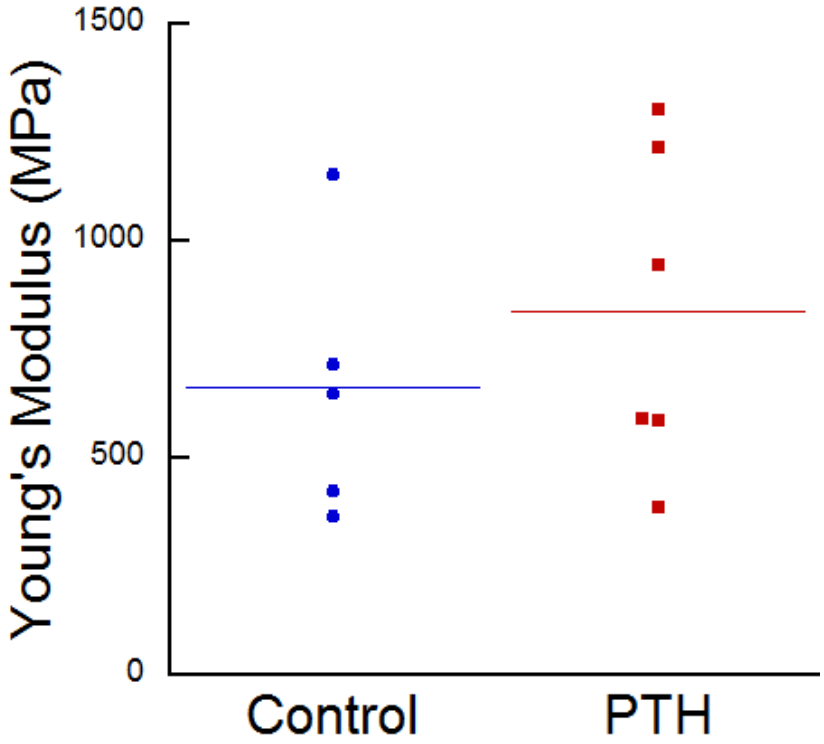

Figure 3.1: The mean Young's modulus of PTH treated samples was 26.7% greater than control. However, with the sample sizes and variation, no significant differences were detected.

We expected that increases in bone mass would improve mechanical properties of cancellous bone of PTH treated sheep compared to those of Control. However, the range in BV/TV across both groups was small, and no correlations were present between BV/TV and mechanical properties (Young's modulus, yield strength and ultimate strength) (Fig. 3.2).

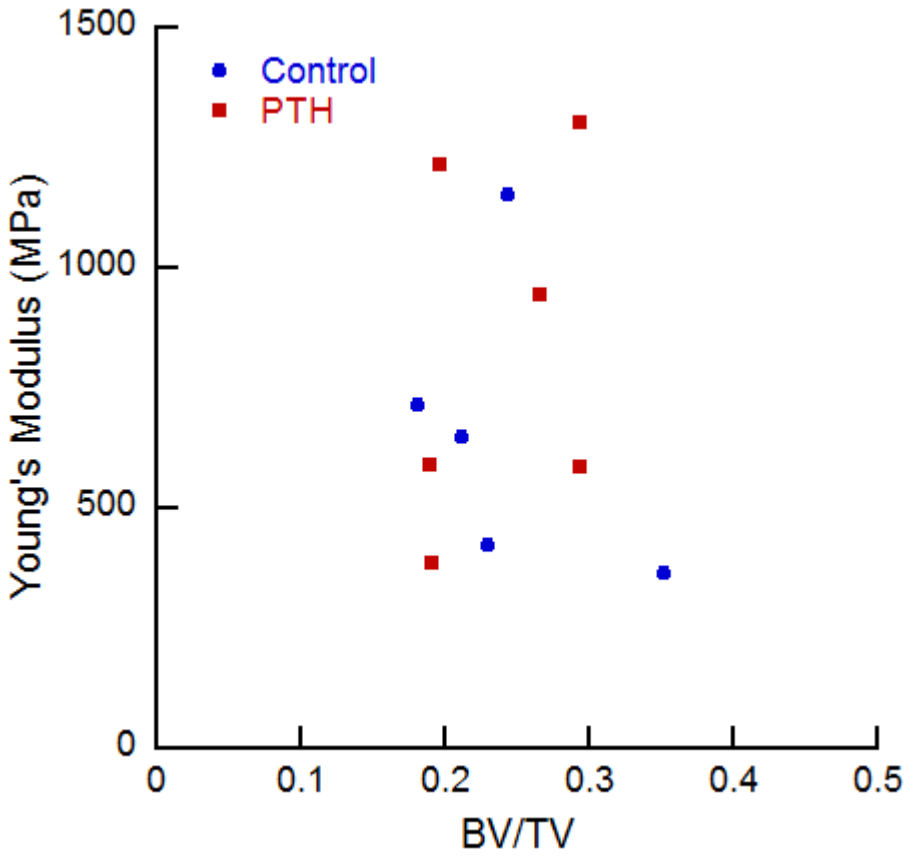

Figure 3.2: No correlation between Young's modulus and BV/TV. BV/TV in PTH-treated group was not different than that of the Control group. Accordingly, no differences in Young's modulus between treatment groups were detected.

3.4 Discussion

In this study, we investigated the effect of treatment with PTH on the mechanical properties of cancellous bone in a sheep model of osteopenia. No detectable differences in uniaxial compression properties were observed. Mechanical properties are determined by bone mass and tissue material properties. Bone volume fraction (BV/TV) was not significantly different between groups. There may be differences in bone tissue material properties that are not detectable in monotonic compression but are in fatigue or fracture toughness.

Previous studies of the mechanical effects of PTH treatment in bone found improved mechanical properties in the femoral neck of rats [11] and lumbar vertebra of rats [10] and

monkeys [12, 13]. The current study looked at cancellous bone from the distal femur in a sheep model of osteoporosis. We found that PTH treatment for the time period studied did not affect cancellous bone mass or mechanical properties in uniaxial compression. The effects of PTH treatment on bone mass may be greater in other regions of the skeleton or if PTH treatment had been extended for a longer period of time.

The current study has a number of strengths. First, this study used a large animal model of osteoporosis. Large animal models have the advantage that cancellous bone can be mechanically characterized independently of cortical bone. Second, cancellous bone was tested not only in monotonic compression but also fatigue (data not shown). Both uniaxial and fatigue mechanical properties influence fracture risk.

Some limitations have to be considered. First, the bone volume fraction in the distal femur of osteopenic sheep, even with OVX + MA diet (0.18 – 0.35), was greater than that of older adults (0.10-0.15). In addition, the small sample size with the high variation in mechanical properties limited our ability to detect differences in uniaxial compression.

Despite these limitations, the lack of detectable effects of PTH treatment on mechanical properties of cancellous bone of the distal femurs contributes to the understanding of the effect of PTH treatment on bone. Bone mass and tissue material properties influence bone mechanical properties. There were no detectable differences in bone volume fraction between PTH treated and Control samples, and no detectable differences in mechanical properties in uniaxial compression. There may be differences in tissue material properties of PTH treated compared to Control that are not highly influential in monotonic loading; however, can play a role in properties in fatigue or fracture toughness.

Fracture risk is influenced by more than compressive strength. Fatigue and fracture toughness influence fracture risk and can provide explanations for fracture risk not explained by BMD [14]. Compressive strength measures the maximum load the bone tissue can withstand at any single time. However, bone is cyclically loaded and accumulates damage daily. Fracture toughness determines the maximum load a bone can withstand with damage present. Only 41% of vertebral fragility fractures can be explained by a single traumatic event [15]. Therefore, the spectrum of mechanical properties must be considered to capture the full picture of how resistant bone is to fracture.

REFERENCES

[1] P. Pisani, M.D. Renna, F. Conversano, E. Casciaro, M. Di Paola, E. Quarta, M. Muratore, S. Casciaro, Major osteoporotic fragility fractures: Risk factor updates and societal impact, World J Orthop 7(3) (2016) 171-81.

[2] R.M. Neer, C.D. Arnaud, J.R. Zanchetta, R. Prince, G.A. Gaich, J.Y. Reginster, A.B. Hodsman, E.F. Eriksen, S. Ish-Shalom, H.K. Genant, O. Wang, B.H. Mitlak, Effect of parathyroid hormone (1-34) on fractures and bone mineral density in postmenopausal women with osteoporosis, N Engl J Med 344(19) (2001) 1434-41.

[3] Y.B. Jiang, J.J. Zhao, B.H. Mitlak, O.H. Wang, H.K. Genant, E.F. Eriksen, Recombinant human parathyroid hormone (1-34) [Teriparatide] improves both cortical and cancellous bone structure, Journal of Bone and Mineral Research 18(11) (2003) 1932-1941.

[4] R.L. Jilka, R.S. Weinstein, T. Bellido, P. Roberson, A.M. Parfitt, S.C. Manolagas, Increased bone formation by prevention of osteoblast apoptosis with parathyroid hormone, Journal of Clinical Investigation 104(4) (1999) 439-446.

[5] H. Dobnig, R.T. Turner, Evidence That Intermittent Treatment with Parathyroid-Hormone Increases Bone-Formation in Adult-Rats by Activation of Bone Lining Cells, Endocrinology 136(8) (1995) 3632-3638.

[6] C.M. de Bakker, A.R. Altman, W.J. Tseng, M.B. Tribble, C. Li, A. Chandra, L. Qin, X.S. Liu, muCT-based, in vivo dynamic bone histomorphometry allows 3D evaluation of the early responses of bone resorption and formation to PTH and alendronate combination therapy, Bone 73 (2015) 198-207.

[7] C.P. Jerome, D.B. Burr, T. Van Bibber, J.M. Hock, R. Brommage, Treatment with human parathyroid hormone (1-34) for 18 months increases cancellous bone volume and improves trabecular architecture in ovariectomized cynomolgus monkeys (Macaca fascicularis), Bone 28(2) (2001) 150-159.

[8] N.E. Lane, J.M. Thompson, G.J. Strewler, J.H. Kinney, Intermittent Treatment with Human Parathyroid-Hormone (Hpth[1-34]) Increased Trabecular Bone Volume but Not Connectivity in Osteopenic Rats, Journal of Bone and Mineral Research 10(10) (1995) 1470-1477.

[9] L. Zhang, H.E. Takahashi, J. Inoue, T. Tanizawa, N. Endo, N. Yamamoto, M. Hori, Effects of intermittent administration of low dose human PTH(1-34) on cancellous and cortical bone of lumbar vertebral bodies in adult beagles, Bone 21(6) (1997) 501-506.

[10] C. Ejersted, T.T. Andreassen, E.M. Hauge, F. Melsen, H. Oxlund, Parathyroid hormone (1-34) increases vertebral bone mass, compressive strength, and quality in old rats, Bone 17(6) (1995) 507-511.

[11] C.H. Sogaard, T.J. Wronski, J.E. Mcosker, L. Mosekilde, The Positive Effect of Parathyroid-Hormone on Femoral-Neck Bone Strength in Ovariectomized Rats Is More Pronounced Than That of Estrogen or Bisphosphonates, Endocrinology 134(2) (1994) 650-657.

[12] M. Sato, M. Westmore, J. Clendenon, S. Smith, B. Hannum, G.Q. Zeng, R. Brommage, C.H. Turner, Three-dimensional modeling of the effects of parathyroid hormone on bone distribution in lumbar vertebrae of ovariectomized cynomolgus macaques, Osteoporosis Int 11(10) (2000) 871-880.

[13] J. Fox, M.A. Miller, M.K. Newman, C.H. Turner, R.R. Recker, S.Y. Smith, Treatment of skeletally mature ovariectomized rhesus monkeys with PTH(1-84) for 16 months increases bone formation and density and improves trabecular architecture and biomechanical properties at the lumbar spine, Journal of Bone and Mineral Research 22(2) (2007) 260-273.

[14] C.J. Hernandez, M.C. van der Meulen, Understanding Bone Strength Is Not Enough, J Bone Miner Res 32(6) (2017) 1157-1162.

[15] C. Cooper, E.J. Atkinson, W.M. Ofallon, L.J. Melton, Incidence of Clinically Diagnosed Vertebral Fractures - a Population-Based Study in Rochester, Minnesota, 1985-1989, Journal of Bone and Mineral Research 7(2) (1992) 221-227.

CHAPTER 4

SUMMARY AND DISCUSSION

Fragility fractures are associated with high morbidity. An estimated 9 million people worldwide suffer from a fragility fracture each year. Some populations have increased risk of fragility fractures. Obesity is associated with increased risk of fragility fracture that is not explained by BMD. Obesity is a common precursor for metabolic syndrome; therefore, metabolic syndrome may contribute to increased risk of fracture. Osteoporosis is a metabolic bone disease that is associated with high risk of fragility fractures. PTH is an anabolic drug to treat osteoporosis and reduce the risk of fracture. Here, I characterized the bone phenotype of the TLR5KO mice and determined the effect of PTH treatment on mechanical properties in compression of cancellous bone in a sheep model of osteopenia.

4.1 Bone Phenotype of TLR5KO mice

We characterized the bone phenotype of the TLR5KO mice. We found that the TLR5KO was characterized by impaired cortical bone tissue material properties compared to those of WT. Male and female TLR5KO mice both exhibited this phenotype. There were age and sex dependencies on the effect of mouse strain on appositional growth. Whole bone mechanical strength is known to contribute to resistance to fracture [1]. Whole bone mechanical strength is determined by bone morphology and tissue material properties. At 10, 16 and 20 weeks, bone morphology of the TLR5KO mice compensated for the impaired tissue material properties to maintain whole bone bending strength compared to that of WT. However, at 55 weeks, whole bone bending strength of TLR5KO mice was reduced compared to that of WT. Bone mass accumulation in the TLR5KO male mice at 55 weeks is reduced compared to that of WT due to increased endosteal resorption. These findings suggest that metabolic syndrome may provide an

explanation of why some populations of people have increased risk of fracture beyond what would be expected given BMD.

4.2 Bone mechanical properties of PTH treated osteoporotic sheep

We tested the effect of PTH treatment on cancellous bone mechanical properties in compression. The mean Young's modulus of PTH treated sheep was 26.7% greater compared to WT. There was no effect of treatment detected in the cancellous bone from the distal femur mechanical properties in monotonic compression possibly due to the small sample size and high variation. In the larger study, treatment affected cancellous bone mechanical properties in fatigue. Both monotonic and fatigue properties influence fracture risk.

4.3 Synthesis

The objective of this work was to assess the mechanical properties of cortical bone in a mouse model of metabolic syndrome and cancellous bone in a sheep model of osteopenia. The toll-like receptor 5 deficient (TLR5KO) mouse is a novel model of metabolic syndrome. The metabolic syndrome in TLR5KO mice developed as a result of alterations to the gut microbiome. In Aim 1, we found that TLR5KO mice had impaired cortical bone tissue material properties compared to that of WT. The use of a sheep model of osteopenia helps fill the need for large animal studies in characterizing the effect of PTH treatment on mechanical properties of cancellous bone. Although no significant differences were detected in monotonic compression loading of cancellous bone, there was an effect of treatment on the fatigue mechanical properties of cancellous bone.

REFERENCES

[1] C.J. Hernandez, T.M. Keaveny, A biomechanical perspective on bone quality, Bone 39(6) (2006) 1173-81.

APPENDIX

Body mass adjusted TLR5KO bone size and mechanical properties

Bone geometry parameters are often adjusted for body size to account for differences in body size between mouse strains. Combining data from male and female mice or mice of different ages is not recommended [1]. Body mass adjustments were performed separately for each age/sex pair using the following equation (Eq. 1).

$$\text{Adjusted Bone trait}_{ijkl} = \text{Bone trait}_{ijkl} - \text{Slope of Bone Trait with Body Mass}_{ijk} * \left(\text{Body Mass}_{ijkl} - \text{Average Body Mass}_{ijk}\right) \quad (1)$$

in which i is the sex, j is the age, k is the genotype and l refers to a specific mouse. Average body mass was calculated as the average of the mean body masses of WT and TLR5KO mice to avoid bias due to differences in sample size.

Femoral diaphyseal cortical bone morphology is shown. All values have been adjusted for body mass. (Mean ± S.D).

	Age (wks)	10		16		20		55	
		WT	TLR5KO	WT	TLR5KO	WT	TLR5KO	WT	TLR5KO
Male	Femur length (mm)	15.59 ± 0.10	15.37* ± 0.15	16.22 ± 0.18	15.83* ± 0.22	15.81 ± 0.08	15.72 ± 0.22	16.28 ± 0.19	15.82* ± 0.30
	Total area (mm^2)	1.95 ± 0.13	1.97 ± 0.05	1.98 ± 0.12	2.12* ± 0.17	2.10 ± 0.04	1.83* ± 0.11	2.46 ± 0.15	2.28* ± 0.11
	Marrow area (mm^2)	1.08 ± 0.09	1.17 ± 0.06	1.11 ± 0.06	1.17 ± 0.15	1.21 ± 0.03	1.05 ± 0.06	1.41 ± 0.14	1.40 ± 0.09
	Cortical area (mm^2)	0.86 ± 0.07	0.79 ± 0.09	0.87 ± 0.07	0.94 ± 0.06	0.89 ± 0.03	0.78 ± 0.06	1.05 ± 0.10	0.87* ± 0.07
	Moment of Inertia (mm^4)	0.15 ± 0.02	0.14 ± 0.01	0.15 ± 0.02	0.17* ± 0.03	0.17 ± 0.01	0.12* ± 0.02	0.22 ± 0.03	0.17* ± 0.02
Female	Femur length (mm)	15.07 ± 0.21	15.06 ± 0.17	15.72 ± 0.09	15.43* ± 0.28	16.57 ± 0.29	15.73* ± 0.25	-	-
	Total area (mm^2)	1.58 ± 0.08	1.54 ± 0.03	1.52 ± 0.07	1.53 ± 0.09	1.70 ± 0.09	1.52 ± 0.09	-	-
	Marrow area (mm^2)	0.94 ± 0.04	0.93 ± 0.02	0.88 ± 0.08	0.87 ± 0.06	0.93 ± 0.05	0.82 ± 0.07	-	-
	Cortical area (mm^2)	0.64 ± 0.05	0.61 ± 0.05	0.64 ± 0.02	0.66 ± 0.06	0.77 ± 0.05	0.70 ± 0.05	-	-
	Moment of Inertia (mm^4)	0.10 ± 0.01	0.09 ± 0.01	0.09 ± 0.004	0.09 ± 0.01	0.11 ± 0.01	0.10* ± 0.01	-	-

* different from WT ($p < 0.05$)

REFERENCES

[1] K.J. Jepsen, M.J. Silva, D. Vashishth, X.E. Guo, M.C. van der Meulen, Establishing biomechanical mechanisms in mouse models: practical guidelines for systematically evaluating phenotypic changes in the diaphyses of long bones, J Bone Miner Res 30(6) (2015) 951-66.